Progress In Electromagnetics Research M, Vol. 108, 79–88, 2022

Performance Prediction of Directed Energy Weapons

Graham V. Weinberg*

Abstract—Directed energy weapons provide a number of useful functions for the modern fighting force, and hence it is useful to produce a framework in which such a weapon's performance can be predicted. Towards this objective this paper introduces a new stochastic model to determine the number of targets defeated by a directed energy weapon over a given time interval. The key to this is to introduce a general queueing model, where arrivals are modelled by a renewal process, and the service time of a target being affected by the weapon is related to its probability of defeat. The queue is assumed to have an infinite capacity, and it is shown how the waiting time of detected threats can be modelled by an auxiliary delay process. A random variable counting the number of targets processed by the queue is then defined. Several functions constructed from this random variable will be investigated in order to identify a suitable metric for assessing performance. In order to facilitate this an example where a high energy laser is used for threat defeat is examined to investigate the utility of the identified performance metrics. As will become apparent, the modelling framework has considerable utility due to the fact that it can be used for performance prediction of any weapon system where an arrival process of threats and corresponding probability of defeat can be specified.

1. INTRODUCTION

Directed energy weapons (DEWs) are an emerging disruptive technology that has utility for a number of important military applications [1, 2]. These applications include disruption of airborne threats, such as unmanned aerial vehicles and missiles, as well precision strikes against remote targets. The two main categories of DEWs are high energy lasers (HELs) and high power radio frequency (HPRF) effectors. HEL DEWs have shown potential for ground-based air defence against airborne threats as mentioned above [3, 4], while HPRF DEWs can also be used for similar applications [5, 6]. While a HEL DEW must be coordinated with a tactical radar in order to direct its beam at the threat for a sufficient dwell time, an HPRF DEW has the advantage that it can deliver a wider beam of energy to provide instantaneous regional defence. However, there are tradeoffs in the latter which can be clarified through the differences between these two DEWs. The main difference between HEL and HPRF DEWs results from the way in which energy is concentrated onto a target, and the effect that it is attempting to induce. A HEL DEW focuses a narrow beam of energy onto a target in order to deliver a thermal disruption to it. However, the beam is attenuated by a number of environmental factors which can result in jittering and distortion of the beam. The consequence of this is that in certain environmental situations the HEL beam may diverge from its target or not deliver sufficient power to cause thermal disruption [7, 8].

HPRF DEWs operate at larger wavelengths than HEL DEWs, and consequently require much larger resonators or antennae to deliver energy onto a target. HPRF DEWs aim to disrupt a target by disabling its electronics, through the delivery of pulsed power which can cause coupling into the target's internal systems. However, in order to deliver sufficiently high powered pulsed energy onto a target,

Received 12 November 2021, Accepted 7 February 2022, Scheduled 16 February 2022
* Corresponding author: Graham V. Weinberg (graham.weinberg@dst.defence.gov.au).
The author is with the Defence Science and Technology Group, Australia.

the size and weight of the resultant effector make it difficult to deploy except in fixed locations or by reducing its output power to make the resultant effector more portable [9, 10].

Due to the importance of DEWs it is useful to produce a framework in which their performance can be analysed in ideal situations. Hence the purpose of the current paper is to develop this capability by introducing a novel approach for performance prediction. This objective will be achieved by introducing a queueing theory model for performance analysis of DEWs. This interpretation views the DEW effector as the queue server, and detected threats are viewed as customers allocated to the queue. The time taken for a threat to enter service is modelled by the customer's delay in the queue. Arrivals to the queue are interpreted as realisations of a general renewal process. The output of the queue can be used to count the number of threats the DEW has defeated by a given time. This then permits the determination of measures of effectiveness of a DEW relative to its operational characteristics and the scenario in which it is functioning.

The general results derived will then be applied to a HEL DEW with parameters sourced from the open literature, to illustrate how DEW performance prediction can be quantified using this approach. It is worth remarking that the general methods can also be applied to HPRF DEWs; a suitable reference which contains a relevant expression for the probability of HPRF DEW defeat of a target can be found in [11]. Additionally, the framework developed can also be applied to any situation where a weapon system faces a series of targets, provided that a suitable expression for the arrival process and probability of defeat can be stipulated.

2. THE QUEUEING THEORY MODEL

A useful reference on the theory of queues is [12], from which some of the development has been motivated. The queueing model has what is referred to as a G/G/1 structure, with an arbitrary renewal process governing the arrivals of threats into the system, and with a service distribution determined from the probability of disruption of the particle by the DEW effector. When a threat arrives it is either served immediately, or it experiences a delay. In the case where a series of threats are detected simultaneously they will be passed into the queue in an arbitrary order and then will be processed individually. Once threats are placed in the queue they remain there until they are served, and the queueing discipline is first come first served. It is also assumed that the queue has an infinite capacity, although in practice only a finite number of threats will be present. One important consideration is that while a threat is in the queue its distance, in terms of the physical combat space relative to the effector, will reduce with time, and so by the time it enters service this must be taken into consideration.

Figure 1 provides an illustration of the combat scene under consideration. Here it is assumed that the HEL DEW is deployed on a land-based platform and is facing a series of threats. In Figure 1 the effector is denoted as E and is located at the origin of the Cartesian coordinate system. There are five threats $(V_1, V_2, \ldots, V_5)$, where the index denotes the order in which the respective threat has arrived. Figure 2 provides an illustration of the queueing theory model adopted for this analysis.

Suppose that the arrival of threats into the system is through a renewal process with interarrival times given by $\{X_j, j \in \mathbb{N} := \{1, 2, \ldots\}\}$, which consists of non-negative independent and identically distributed random variables. Then time of arrival of the nth threat is given by

$$S_n = \sum_{i=1}^{n} X_i \tag{1}$$

for $n \in \mathbb{N}$. Consequently, the random variable defined by $N(t) = \sup_{n \in \mathbf{N}}\{S_n \leq t\}$ counts the number of arrivals by time t. Examples of renewal processes include the Poisson, where the interarrival times are exponentially distributed [13].

Suppose that the service time of particle n is Y_n, and that D_n is the delay or waiting time of the nth particle in the queue. This particle spends a time $D_n + Y_n$ while in the queue, and the next particle arrives at an interarrival time of X_{n+1} after particle n. Hence the delay that this new particle experiences is

$$D_{n+1} = \begin{cases} D_n + Y_n - X_{n+1} & \text{if} \quad D_n + Y_n \geq X_{n+1} \\ 0 & \text{otherwise,} \end{cases} \tag{2}$$

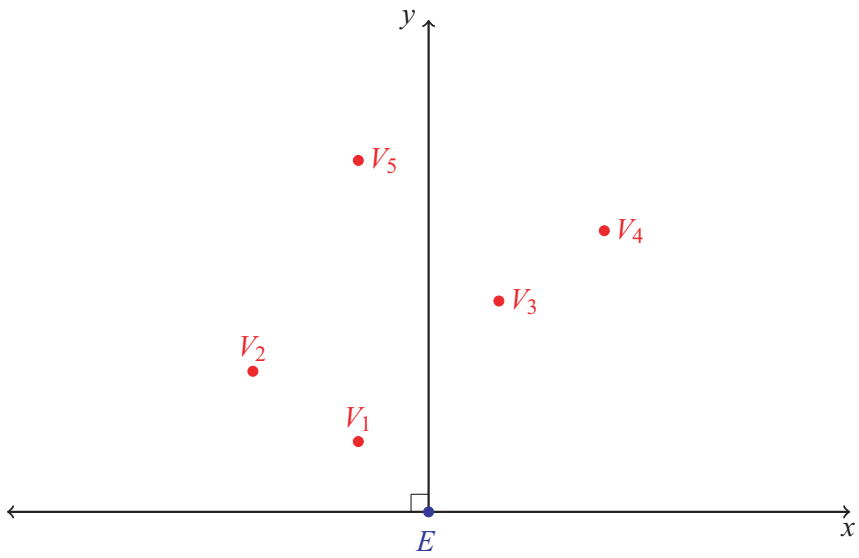

Figure 1. An illustration of the combat scene, where a series of threats arrive sequentially and then are targeted by an effector. The threats are denoted V_j where the index indicates its order in terms of arrival. The effector is labelled E and is shown at the origin. Once threats have been detected it can be assumed that their position relative to E is known, as well as their relative speed.

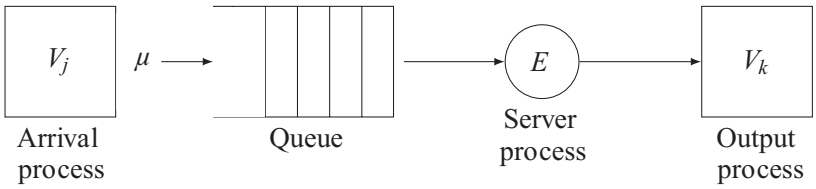

Figure 2. The process viewed as a queueing theory model. Threats arrive into the system, at a rate of μ, and then are placed into the queue, in a first come first serve protocol. Once a threat has been served it is considered a part of the output process. The latter counts the number of threats defeated by a given time.

(see [12]). Based upon Eq. (2) it follows that

$$D_{n+1} = \max\{0, D_n + Y_n - X_{n+1}\} \tag{3}$$

for $n \geq 1$ and $D_1 := 0$ since the first particle to arrive will not experience a delay but is immediately served. One can in principle solve Eq. (3) recursively. However, this is not required in the current context.

Observe that the random variable $S_n + D_n + Y_n$ is the time at which the nth threat exits the queue, relative to time beginning at zero. Hence the random variable

$$M(t) = \sup_{n \in \mathbf{N}} \{S_n + D_n + Y_n \leq t\} \tag{4}$$

counts the number of threats that have passed through the queue by time t. Therefore, in specific numerical examples, if one has *a priori* knowledge of the number of threats that the DEW is facing, then Eq. (4) can be used to assess the performance of the DEW in defeating the threats before they would arrive at their target (the DEW's host platform) in the case that they are not intercepted. Consequently it is important to determine a metric, based upon Eq. (4), which permits performance analysis to be undertaken.

Note that if $M(t) \geq m$, for some $m \in \mathbb{N}$, then this will imply that $S_m + D_m + Y_m \leq t$. Similarly, if the latter holds then this will also imply that the former is also valid. Hence these two events are

equivalent, and it follows that

$$\mathbb{P}(M(t) \geq m) = \mathbb{P}(S_m + D_m + Y_m \leq t). \tag{5}$$

It follows that Eq. (5) can be used to determine the complementary distribution function of $M(t)$ by evaluating its right hand side. The way in which this can be evaluated is to apply a Monte Carlo simulation [14], since it will be analytically complicated to evaluate Eq. (5) directly. However, simulation of the random variables S_m, D_m and Y_m is manageable.

In order to derive the point probabilities of $M(t)$ observe that

$$\mathbb{P}(M(t) \geq m) - \mathbb{P}(M(t) \geq m+1) = \mathbb{P}(M(t) = m) \tag{6}$$

and Monte Carlo estimation of Eq. (5) can then be applied to Eq. (6).

It is also possible to compute the mean number of threats defeated as a function of time, by utilising Eq. (6). Hence one can consider

$$\mathbb{E}(M(t)) = \sum_{m=1}^{\infty} m\mathbb{P}(M(t) = m). \tag{7}$$

The three functions (5), (6), and (7) can therefore be utilised as metrics to assess a given DEW's performance. These three metrics will hence be examined in the numerical example to follow.

As an aside, it is worth noting that this model developed for performance prediction is under ideal situations. Hence in practice, a mismatch in modelling assumptions will necessarily introduce modelling errors. In addition to this, it is assumed that the DEW platform is not subjected to other effectors which may have an impact on performance.

Prior to considering a specific DEW some comments on the evaluation of these metrics, through simulation of their components, are merited. The renewal process can be simulated through assumptions imposed on the interarrival times. Service times can be simulated through an equivalence of it to the probability of disruption of a particle as follows. Suppose that the probability that particle j is eliminated by the server (or DEW effector) by time t is $\phi_j(t)$. Then the probability that Y_j exceeds t is equivalent to the probability that the particle is not processed by queue server by time t. Hence it can be shown that

$$\mathbb{P}(Y_j > t) = 1 - \phi_j(t). \tag{8}$$

Consequently Eq. (8) characterises the time it takes for the queue server to process the threat in the queue. Additionally, this expression is in a suitable form to simulate the service times by using the inverse cumulative distribution function transform method [15]. The delays can also be simulated from the interarrival times and service times through Eq. (3).

The next section will illustrate the application of the queueing model to performance prediction of a HEL DEW.

3. EXAMPLE OF PERFORMANCE ANALYSIS

The context for the example considered is a land-based armoured fighting vehicle with a HEL DEW, facing a series of homogeneous threats, as in the studies reported in [11, 16]. Here it is assumed that a series of 10 threats are fired toward the DEW's platform, and that each threat travels at a constant speed of 50 metres per second. From a radar perspective, it is assumed that the threats have a small radar cross section (0.1 metre square at X-band: see [16]). Once a threat appears (in terms of being detected by the host platform) it is assumed that it will take 120 seconds to reach its target if not intercepted and destroyed. The arrival of these threats is modeled as a Poisson process with a given mean rate of arrivals, to be clarified in the two cases considered. The HEL DEW's operational parameters have been selected by consideration of parameters for HELs available in the open literature. The HEL is assumed to have a power level of $P_0 = 30\,\text{kW}$ with a duty cycle of $C = 0.5$. Laser propagation factors have been selected from Tables 1 and 2 of [17]. The laser wavelength is $\lambda = 1.045\,\mu\text{m}$; the mechanical jitter angle of the laser beam is $\theta_J = 1$; the intrinsic laser beam quality is $\mathcal{M}^2 = 4$; r_0 is the transverse coherence length associated with turbulence which is given by

$$r_0 = 0.184 \left(\frac{\lambda^2}{c_n^2 R(t)} \right)^{\frac{3}{5}}, \tag{9}$$

where c_n^2 characterises the strength of turbulence and has been selected to be $c_n^2 = 10^{-15}$, and $R(t)$ is the range to the target from the DEW platform. The initial laser spot size is $R_0 = 0.1\,\mathrm{m}$, and the coefficient γ representing atmospheric extinction due to both absorption and scattering, has been selected to be $\gamma = 2 \times 10^{-3} + 1.2 \times 10^{-1}\,\mathrm{km}^{-1}$.

A model for HEL DEW effects, in terms of the probability of disruption of a target, has been developed in [16], based upon these HEL characteristics. It assumes that the HEL dwell time can be modelled by a truncated exponential distribution with parameter μ_τ and that the target has an average illumination area parameter μ_σ. The target vulnerability threshold is assumed to be U, which is the point above which the power density on the target causes a thermal effect.

The threats are assumed to travel at a constant speed toward the effector's platform, so the distance between the latter and the threat is a linear function. Specifically, for a speed of v metres per second and assuming that the threat takes T seconds to reach its target if not intercepted, the distance of the threat from the effector is given by $R(x) = \nu(T - x)$, for $x \leq T$. Based upon [16], the probability of HEL DEW disruption of the target can be shown to be

$$\phi(t) = \frac{\mu_\tau}{1 - e^{-\mu_\tau t}} \int_0^t e^{-\mu_\tau s} e^{-\mu_\sigma \frac{U}{\kappa P_0 C} \frac{\nu^2 (T-t)(T-t+s)}{s}} ds. \tag{10}$$

where $\kappa = 1.8330 \times 10^{-5}$.

Throughout the following it will be assumed that $\mu_\tau = 1/3$ and $\mu_\sigma = ((1.045^2)/9) \times 10^{-7}$, with $U = 10$. The selection for μ_τ is based upon an average HEL DEW dwell time of 3 seconds, while the choice for μ_σ is motivated upon a result in [16] which produces a relationship between the laser and radar wavelengths and a normal to the target's surface area (see [16] for clarification of this). These parameters, as well as the other HEL characteristics described above, can be applied to Eq. (10) directly.

Probabilities associated with the queueing process have been estimated using Monte Carlo simulation with 5000 runs. Since it is assumed that the arrival process is Poisson, the interarrival times are generated by simulating exponential random variables with rate μ, and then applying these to Eq. (1) to generate the arrival times of threats. The service times of threats in the queue are simulated by applying Eq. (10) to Eq. (8) and applying the inverse cumulative distribution simulation technique referred to previously. Delays of threats in queues are simulated by appeal to Eq. (3), observing that $D_1 = 0$. Once a threat enters service it is necessary to adjust the function $R(x) = \nu(T - x)$ utilised in Eq. (10). Note that threat j is detected at time S_j, is traveling at ν metres per second and would take T seconds to strike its intended target if not intercepted. This threat enters service at time $S_j + D_j$, and at time S_j the distance of threat to effector is νT, and at time $S_j + T$ it is zero. Hence it follows that the distance between the effector and this threat is $\nu(S_j + T - t)$ at time t. Based upon this when the threat enters service it is at a distance of $\nu(T - D_j)$ m from the effector. Consequently, relative to the effector, the distance to the threat is $\nu(T - D_j - t)$ m, and the latter can then be applied to Eq. (10) to produce the appropriate probability of disruption.

Tangible examples are now considered. The first example assumes that the interarrival times have a mean rate of unity. Figure 3 plots the probability that $M(t)$ exceeds m, where $m \in \{1, 2, \ldots, 10\}$. Hence it is plotting the probability that at least m threats are defeated as a function of time. Figure 4 plots the three cases $m \in \{1, 5, 10\}$ for clarity. Clearly the probability that at least one threat is defeated exceeds all the other cases, while $m = 10$ corresponds to all threats defeated. By time 140 seconds all the threats have almost certainly been defeated.

Figure 5 provides a plot of the point probabilities that $M(t) = m$ for the three cases in Figure 4. The figure provides an interesting perspective of the situation. The two cases $m = 1$ and $m = 5$ show that as time evolves, it is not likely that only a particular number of threats are defeated and that as time continues these probabilities will unsurprisingly limit to zero. This is because as time increases it is likely that more threats are defeated. The limiting case (where $m = 10$) will have the largest point probability over time because it is more likely that all the threats are defeated. From a performance prediction perspective, this plot is not extremely useful and is only included to provide an example of point probabilities for this analysis.

Figure 6 is for the case where the mean arrival rate has been increased to 10 per second, and Figure 7 shows the three cases ($m = 1$, $m = 5$, and $m = 10$). Due to the increase in the arrival rate the main difference in this case is that it generally takes longer to eliminate the threats.

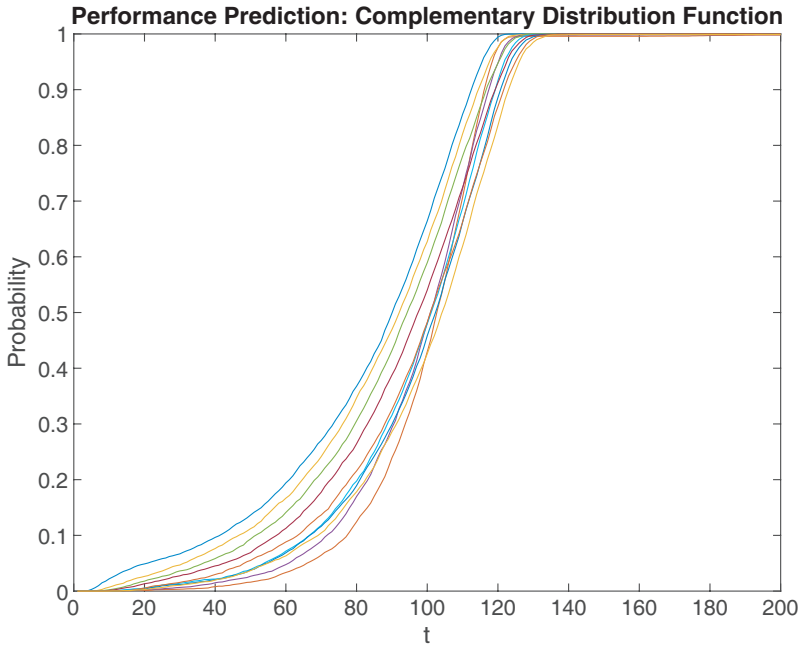

Figure 3. Plots of $\mathbb{P}(M(t) \geq m)$ where $m \in \{1, 2, \ldots, 10\}$. The left most curve is for the case where $m = 1$ while the right most curve corresponds to $m = 10$. Figure 4 provides clarification of this (curves not labelled for brevity). This plot is for the situation where the arrival process has a mean arrival rate of unity.

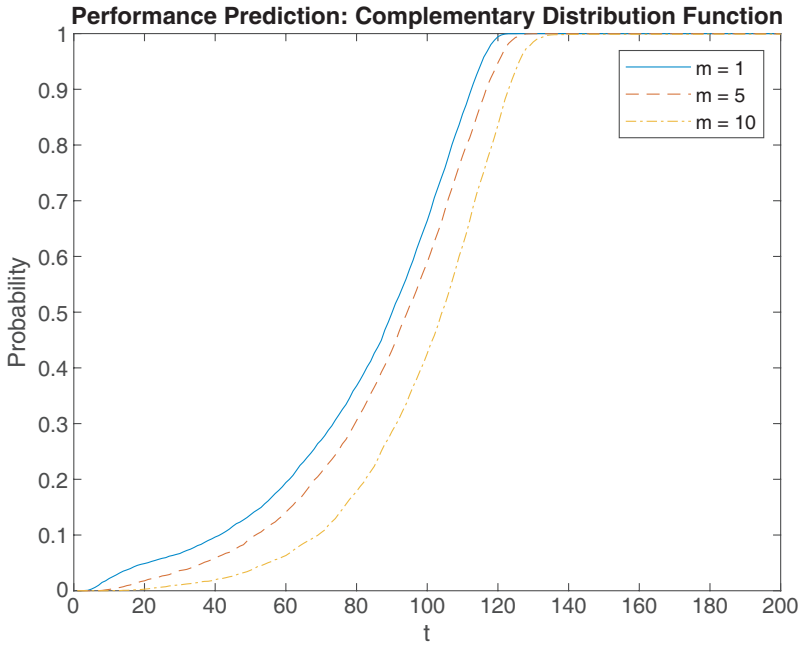

Figure 4. A subplot based upon Figure 3 of $\mathbb{P}(M(t) \geq m)$ for the three cases $m = 1$, 5 and 10.

From the perspective of performance prediction comparisons, the two cases considered above can be compared through a pairwise comparison of Figures 3 and 6, or through Figures 4 and 7. However, it would be more useful if the results of each case could be compressed to allow comparison more readily. In order to achieve this aim, one can plot the mean of the number of threats defeated as a function of

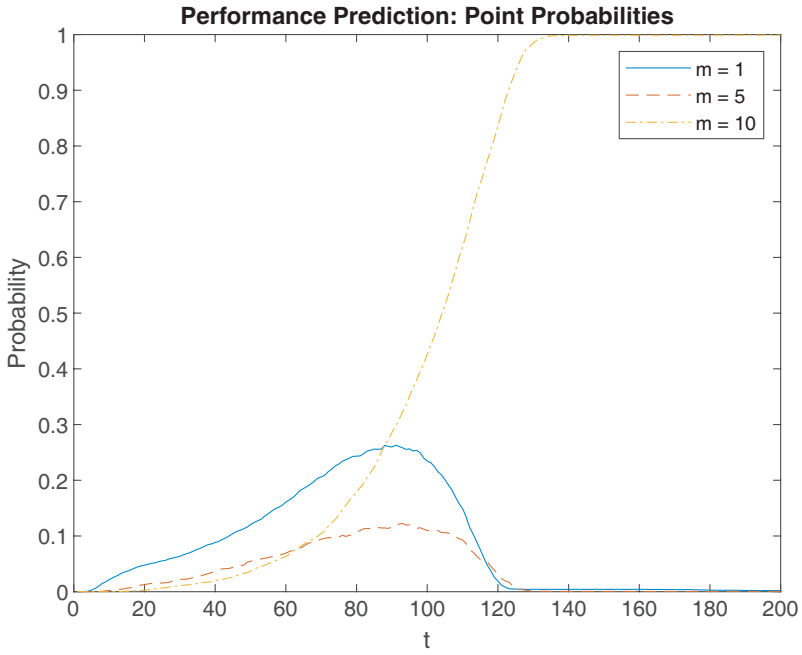

Figure 5. Plots of the point probabilities $\mathbb{P}(M(t) = m)$ for the three cases where $m = 1$, 5 and 10. The process arrival rate is unity.

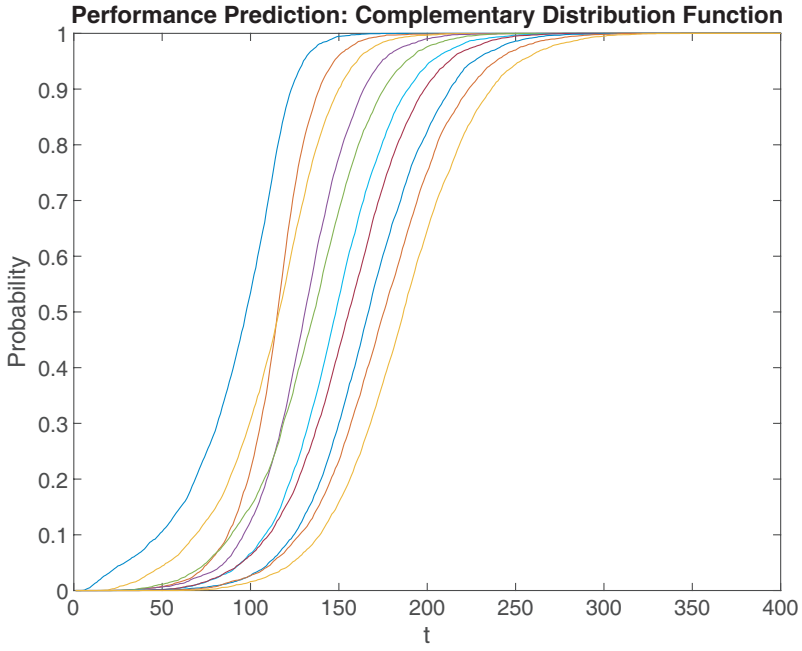

Figure 6. A plot of the complementary cumulative distribution function $\mathbb{P}(M(t) \geq m)$ over the same range of m as for Figure 3 except with a mean arrival rate of 10.

time. This then compresses the results for an example to a single performance curve. Figure 8 plots this mean for the two examples considered above (Example 1 is for an arrival rate of unity, while Example 2 is for an arrival rate of 10). One can see that the mean number of threats defeated will decrease as the arrival rate increases, which is plausible. Hence one can utilise the mean number of threats defeated as a suitable DEW performance metric.

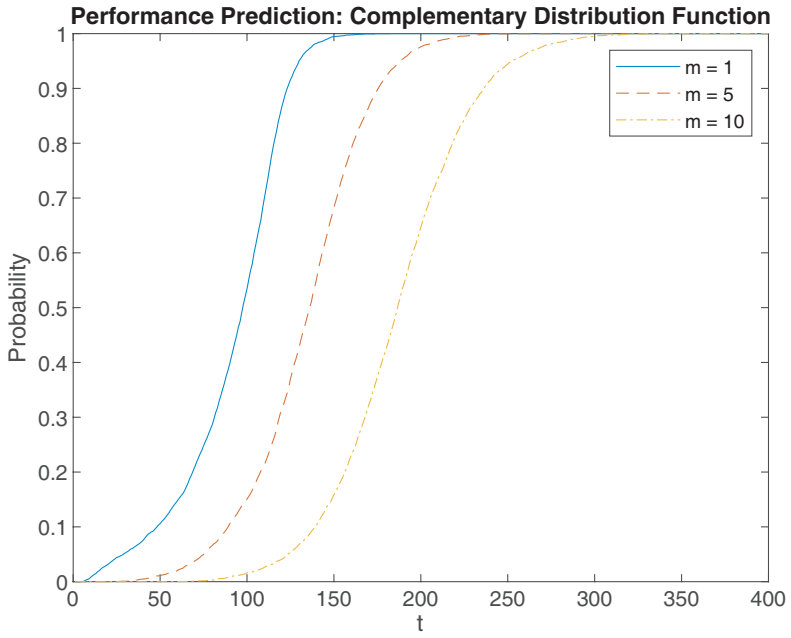

Figure 7. Subplot of Figure 6 over a smaller subset of m.

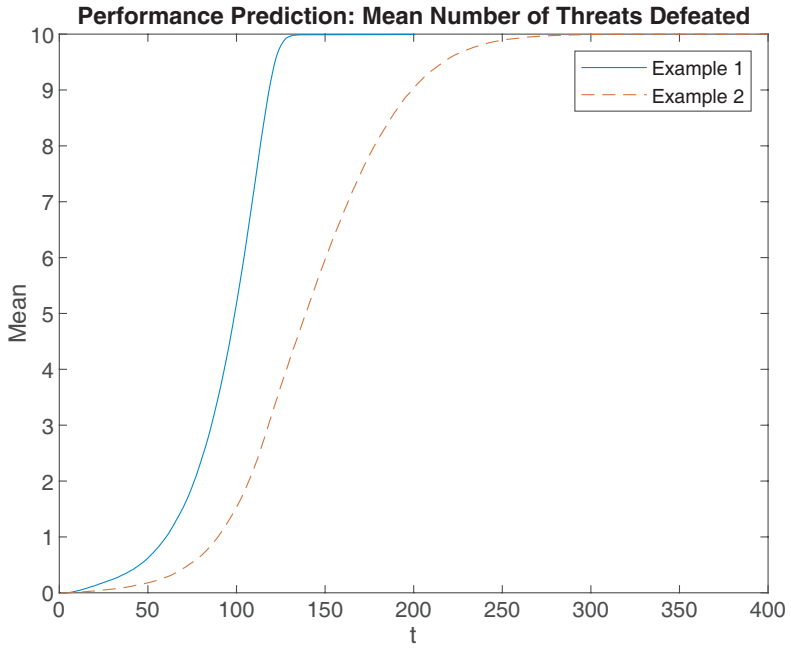

Figure 8. A plot of the mean number of threats defeated, as a function of time, for the two examples considered. This enables an easier comparison between the two different cases, where the key difference is the threat rate of arrivals. This also suggests that the mean number of threats defeated can be used as a performance metric. Example 1 has a mean arrival rate of unity, while Example 2 is for 10 arrivals per second.

The plot in Figure 8 illustrates how one can apply the methodology to undertake performance analysis and prediction of different HEL DEWs operating in the same setting. In the current case it was shown how the arrival rate can affect the rate at which threats are defeated. This approach can also be used to analyse other factors, both from the threat perspective and DEW operational characteristics.

4. CONCLUSIONS AND FURTHER WORK

The purpose of this study was to develop a framework in which DEW performance prediction can be undertaken. This was based upon interpreting the problem from a queueing theory perspective. The key to this was to interpret the DEW effector as a queue server, and detected threats as customers in the queue. It was shown how the number of threats defeated by a given time could be related to functions of the queue.

It is worth observing that the novel framework is general and can be applied to performance prediction of any weapon system where the arrivals can be modelled by a renewal process and provided that an expression for the probability of defeat is available. The model itself has been developed with land-based DEW applications. However, it can be applied to both airborne and maritime systems.

Analysis of the outputs of the queue indicated that a suitable way in which to undertake performance predictions was to analyse the mean number of threats defeated as a function of time. This was illustrated using a land-based application, where the arrival rate of threats was varied through two examples. This methodology can be applied to assess a DEW's operational effectiveness in a given scenario by allowing variation of its parameter sets and plotting the corresponding mean number of threats defeated.

This approach can be seen to extend quite readily to the case where there are a number of DEW effectors, facing a series of threats. Once threats are detected they can then be allocated to what is determined to be the most appropriate effector (queue) where it will await until it is eliminated. Thus this is suggesting that a network of queues approach could be used to model the case where there is more than one DEW effector. The construction of this novel framework will permit the performance prediction of a wide range of weapon systems used across the defence forces. This weapon performance prediction capability will form the basis for future research.

REFERENCES

1. Nielsen, P. E., *Effects of Directed Energy Weapons*, National Defence University, Washington, 1994.
2. Deveci, B. M., "Directed-energy weapons: Invisible and invincible?," Master of Science in Electronic Warfare Systems Engineering. Naval Postgraduate School, Monterey, 2007.
3. Hafften, M. and R. Stratton, "High energy laser weapon integration with ground vehicles," NATO Report presented to *RTO AVT Symposium*, RTO-MP-AVT-108, 2004.
4. "The high energy laser: Weapon of the future already a reality at Rheinmetall," Product Description Sheet, 2021.
5. Radasky, W. A., "The threat of Intentional Interference (IEMI) to wired and wireless systems," *17th International Zurich Symposium on Electromagnetic Compatibility*, 2006.
6. Radasky, W. A., C. E. Baum, and M. W. Wik, "Introduction to the special issue on High Power Electromagnetics (HPEM) and Intentional Electromagnetic Interference (IEMI)," *IEEE Transactions on Electromagnetic Compatibility*, Vol. 46, 314–321, 2004.
7. Gebhardt, F. G., "High power laser propogation," *Applied Optics*, Vol. 15, No. 6, 1479–1493, 1976.
8. Cook, J. R., "Atmospheric propogation of high energy lasers and applications," *American Institute of Physics*, Vol. 766, No. 58, 2005.
9. Braidwood, S. and K. Hong, "Stopping car engines using high power electromagnetic pulses," *International Conference on Electromagnetics in Advanced Applications*, 2010.
10. Simon, M. D., "Solid-state high power radio frequency directed energy systems in support of USMC force protection operations," Masters Thesis, Naval Postgraduate School, Monterey, 2015.
11. Weinberg, G. V., "Quantification of combat team survivability with high power RF directed energy weapons," *Progress In Electromagnetics Research M*, Vol. 102, 1–11, 2021.
12. Ross, S. M., *Stochastic Processes*, Wiley, 1996.
13. Durrett, R., *Probability: Theory and Examples*, Wadsworth Publishing Company, Duxbury, 1996.
14. Rubinstein, R. Y., *Simulation and the Monte Carlo Method*, Wiley, 1981.
15. Ross, S. M., *Simulation*, Academic Press, 2002.

16. Weinberg, G. V. and M. M. Kracman, "Armoured fighting vehicle team performance prediction against missile attacks with directed energy weapons," ArXiv Preprint, arXiv:2106.14381v1, 2021.
17. Sprangle, P., J. Penano, and B. Hafizi, "Optimum wavelength and power for efficient laser propagation in various atmospheric environments," Naval Research Laboratory Report, NRL/MR/6790-05-8907, 2005.